

# Does the aortic annulus undergo conformational change throughout the cardiac cycle?

## A systematic review

Dominika Suchá<sup>1†\*</sup>, Volkan Tuncay<sup>2†</sup>, Niek H.J. Prakken<sup>3</sup>, Tim Leiner<sup>1</sup>, Peter M.A. van Ooijen<sup>2,3</sup>, Matthijs Oudkerk<sup>3</sup>, and Ricardo P.J. Budde<sup>1</sup>

<sup>1</sup>Department of Radiology, University Medical Center Utrecht, Heidelberglaan 100, 3508 GA, Utrecht, The Netherlands; <sup>2</sup>Center for Medical Imaging – North East Netherlands (CMINEN), University Medical Center, Groningen, The Netherlands; and <sup>3</sup>Department of Radiology, University Medical Center, Groningen, The Netherlands

Received 13 May 2015; accepted after revision 2 August 2015; online publish-ahead-of-print 15 September 2015

Accurate annular sizing in transcatheter aortic valve implantation (TAVI) planning is essential. It is now widely recognized that the annulus is an oval structure in most patients, but it remains unclear if the annulus undergoes change in size and shape during the cardiac cycle that may impact prosthesis size selection. Our aim was to assess whether the aortic annulus undergoes dynamic conformational change during the cardiac cycle and to evaluate possible implications for prosthesis size selection. We performed a systematic search in PubMed and Embase databases and reviewed all available literature on aortic annulus measurements in at least two cardiac phases. Twenty-nine articles published from 2001 to 2014 were included. In total, 2021 subjects with and without aortic stenosis were evaluated with a mean age ranging from  $11 \pm 3.6$  to  $84.9 \pm 7.2$  years. Two- and three-dimensional echocardiography was performed in six studies each, magnetic resonance imaging was used in one and computed tomography in 17 studies. In general, the aortic annulus was more circular in systole and predominantly oval in diastole. Whereas the annular long-axis diameter showed insignificant change throughout the cycle, the short-axis diameter, area, and perimeter were significantly larger in systole compared with diastole. Hence, the aortic annulus does undergo dynamic changes during the cardiac cycle. In patients with large conformational changes, diastolic compared with systolic measurements can result in undersizing TAVI prostheses. Due to the complex annular anatomy and dynamic change, three-dimensional assessment in multiple phases has utmost importance in TAVI planning to improve prosthesis sizing.

### Keywords

Aortic annulus • Conformational change • Imaging parameter • TAVI sizing

## Introduction

In the elderly, the prevalence of moderate-to-severe aortic stenosis (AS) is  $\sim 3\%$ .<sup>1</sup> About half of all patients with severe AS are referred for surgical aortic valve replacement (AVR).<sup>2</sup> For selected high-risk patients, transcatheter aortic valve implantation (TAVI) has become a successful alternative to conventional valve surgery.<sup>3,4</sup>

In conventional AVR, the appropriate size of the prosthesis is determined by direct measurements of the annulus during surgery. In TAVI, assessment of the annular and prosthetic size relies entirely on preprocedural and/or periprocedural imaging. Precise aortic root measurement is essential for choosing the correct prosthesis size to minimize the risk of complications such as significant ( $>$ mild) paravalvular regurgitation, which has been reported in 1–39%

of TAVI patients.<sup>5–7</sup> Measurements of the aortic annulus were originally performed using transthoracic or transesophageal two-dimensional echocardiography (TTE and TEE, respectively). However, studies have found the aortic annulus to often have an ellipsoid shape rather than a circular structure.<sup>8–10</sup> Hence, three-dimensional echocardiography or computed tomography (CT) allows for more accurate assessment of the shape and size of the annulus by providing images in any desired imaging plane.

The ascending aorta is known to undergo conformational changes during the cardiac cycle.<sup>11,12</sup> However, no consensus exists whether such changes are also present in the aortic annulus and in what way. If the annulus does undergo significant dynamic changes, this may affect selection of the most optimal cardiac phase for measurement and improve prosthesis sizing or even prosthesis design.

\* Corresponding author. Tel: +31 887556689; Fax: +31 88 7569589, E-mail: d.sucha@umcutrecht.nl

† These authors contributed equally to this paper.

Published on behalf of the European Society of Cardiology. All rights reserved. © The Author 2015. For permissions please email: journals.permissions@oup.com.

In order to clarify this concern, we conducted a systematic review of all the literature investigating the dynamic behaviour of the aortic annulus using echocardiography, CT, and/or magnetic resonance imaging (MRI).

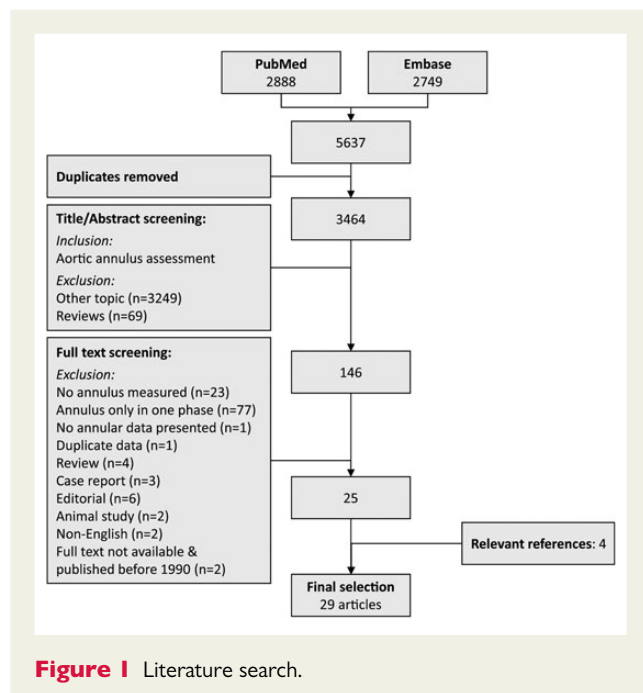
## Methods

### Literature search

PubMed and Embase databases were systematically searched on 25 June 2014 using the search syntax presented in the Appendix. In Embase, we included only articles, articles in press, reviews, and short surveys. No other limitations were applied. Two reviewers (D.S., V.T.) screened all titles and abstracts independently. In total, 5637 articles were found and 2173 duplicates excluded manually (Figure 1).

### Article selection

Only articles aimed at imaging and evaluation of the aortic annulus were included for further screening. In total, 146 articles were selected for full text screening. Both reviewers independently excluded studies evaluating the annulus only in one cardiac phase and articles on other aortic/cardiac dimensions than the annulus. Furthermore, studies on animals, case reports, reviews, editorials, and non-English articles were excluded (Figure 1). A third reviewer (R.B.) settled discordant judgements. Our selection comprised 25 articles on aortic annulus change during the cardiac cycle. References and citations were screened for relevant articles not included in our search. This resulted in four additional articles,<sup>13–16</sup> since annulus as defined in the search syntax was not mentioned in the title/abstract. The final selection included 29 articles.



### Data extraction

We extracted the following data from the selected articles: first author, journal, publication year, number of patients, mean age, gender, number of patients with AS, definition of AS and mean aortic valve area, imaging modalities used for measurements including selected plane and imaging phase, definition of annulus, annulus measurement method (manual, semi-automatic), and annular parameters within the cardiac cycle.

## Results

### Study characteristics

Twenty-nine original articles were included published from 2001 to 2014. Of these, seven evaluated annular dynamic changes in healthy subjects (e.g. no aortic root or valve disease), 10 compared a healthy population with AS patients and 12 studies included only AS patients. In total, 2021 subjects were evaluated with a mean age ranging from  $11 \pm 3.6$  to  $84.9 \pm 7.2$  years. Study and patient characteristics are summarized in Table 1.

### Imaging characteristics

Two-dimensional echocardiography (TTE and/or TEE) in systole and diastole was performed in six studies, all using the parasternal long-axis view. Three-dimensional modalities used for assessment of the annulus were echocardiography (6 studies), MRI (1 study), and CT (17 studies). The CT acquisition protocol comprised retrospective ECG-gating in 15 studies, wide-window (20–90%) dose-modulated prospective ECG-triggering in one study and one study did not specify the CT protocol. Of all three-dimensional modality studies, the MRI and four CT studies evaluated coronal and/or sagittal plane reconstructions<sup>8,10,17–19</sup> and one CT study used an undefined longitudinal view.<sup>20</sup> Reconstructed double oblique images in plane with the aortic annulus were evaluated in 19 studies. Since the annulus is not a true anatomical structure, the exact location of anatomical measurements had to be specified. The aortic annulus was defined in general as a virtual ring at the lowest, most caudal, insertion of the valve leaflets in 22 studies. Two studies measured the ventriculo-arterial junction<sup>20,21</sup> and five studies did not specify aortic annulus.<sup>8,13,18,22,23</sup> Annular measurements were performed semi-automatically in six studies<sup>15,16,23–26</sup> and manually in the remaining 23 studies.

### Deformation during the cardiac cycle

On parasternal long-axis view, the annulus diameter was larger in systole than in diastole in 9 of 10 studies (Table 2, largest mean difference  $2.9 \pm 0.7$  mm). Only two studies performed paired *T*-tests<sup>14,20</sup> of which one found a significant change for TEE-derived diameter throughout the cycle (mean difference  $0.3 \pm 0.7$  mm,  $P = 0.0005$ ).<sup>14</sup> No significant change was shown for TTE-derived diameter measurements.

Results on coronal view measurements were contradictory as the largest annulus diameter was found either in the systolic ( $n = 3$ ) or diastolic phase ( $n = 3$ ) (Table 3). One study evaluated the mean

diameter difference between these phases (0.23 mm) but no statistical significance was reached.<sup>17</sup> However, all results on sagittal view showed larger systolic than diastolic annulus diameters with significant difference (mean 0.42 mm,  $P = 0.008$ ), though tested only by one study<sup>17</sup> (Table 3).

Table 4 shows all diameter measurements acquired using the double oblique in plane view. No evident pattern was found for change in maximal (long axis) annulus diameter since it was largest either in systole or diastole in seven patient groups each. Statistical analysis was performed by seven studies<sup>10,17,25,27–30</sup> but only one found significant differences (mean  $0.3 \pm 2.4$  mm in diastole,  $P < 0.001$ ).<sup>10</sup> In contrast, the minimal (short axis) annulus diameter was largest in systole in the majority of patients (16 study groups) and in diastole in three studies (four patient groups).<sup>22,31,32</sup> The change in diameter (Figure 2) was significant in 11 patient groups<sup>10,17,22,25,27,28,30,33,34</sup> all showing a greater short-axis diameter in systole except for the two groups of Izumi *et al.*<sup>22</sup> Pontone *et al.*<sup>29</sup> did not find significant differences.

The annular area was evaluated in 18 patient groups using double oblique plane reconstructions (Table 5). The majority ( $n = 15$ , 83%) showed the largest area during (early) systole, with a maximal mean difference of  $122 \pm 33$  mm<sup>2</sup> throughout the cardiac cycle.<sup>24</sup> Nine groups were statistically evaluated<sup>16,17,24,29,30,33,35</sup> and the area was significantly larger during systole in seven, during diastole in one and not significantly different in one group.<sup>29</sup>

The annular perimeter was largest during systole in five and during diastole in three groups (Table 6). This was tested and significant in four and one patient group, respectively. The largest mean difference between systole and diastole was  $5.4 \pm 1.5$  mm.<sup>35</sup>

## AS vs. non-stenosis

As presented in Tables 3–6, both non-AS patients (e.g. without aortic root disease) and AS patients showed significant annular change throughout the cycle. Five studies directly compared the extent of conformational change between AS and non-AS patients. Based on longitudinal parasternal view measurements, Shiran *et al.* found similar results for AS and non-AS patients. In contrast, Yoshikawa *et al.* detected significantly less absolute and relative diameter change in AS patients ( $P \leq 0.0027$ ).<sup>23</sup> Furthermore, the diameter reached its maximal value at a later point in the cardiac cycle than in non-AS patients (99 vs. 83 ms from the R-wave, resp.  $P < 0.0004$ ). Using double oblique plane images, Izumi *et al.* also found a significantly smaller annulus diameter deformation in AS patients (2 vs. 8% in controls,  $P < 0.0001$ ).<sup>22</sup> In the study of Hamdan *et al.*, AS patients showed higher annular stiffness compared with healthy subjects, based on the perimeter and left ventricular pressure change (23 vs. 14 MPA, resp.  $P = 0.029$ ).<sup>33</sup> No significant difference was found for dynamic changes between patients with and without aortic valve calcifications.<sup>32</sup>

## Other factors

Aortic root calcifications in general did not show a correlation with annular change<sup>32</sup> or circularity<sup>28</sup> during the cardiac cycle. But the

location of the calcifications was related to annulus area change, showing the least change with both annular and commissural calcifications (6 mm<sup>2</sup>) and the greatest change with only commissural calcifications (23 mm<sup>2</sup>).<sup>32</sup> Only one study evaluated the influence of age on annulus change within the cardiac cycle but found no age effect.<sup>32</sup> In this study, a weak linear correlation was found between diastolic blood pressure and annulus perimeter changes ( $r = -0.25$ ,  $P = 0.01$ ), and between ejection fraction and minimal diameter changes ( $r = -0.22$ ,  $P = 0.03$ ). Another study found the left ventricular outflow tract diameter and stroke volume to be associated with larger changes throughout the cycle.<sup>36</sup>

## Impact on prosthesis sizing

Blanke *et al.* evaluated the annulus in 5% steps throughout the full cardiac cycle and found the selected cardiac phase to affect prosthesis agreement.<sup>35</sup> Selection of the cardiac phase in which the area or perimeter-derived diameter reached its maximal value showed the highest agreement with the selected Edwards Sapien prosthesis and most relative oversizing ( $\pm 10\%$ ). The area and perimeter were largest between 0 and 30% phases of the RR-interval. Measurements obtained in the clinically used 35%-systolic and 75%-diastolic cardiac phase showed only 76% prosthesis agreement (84/110 patients) and less relative oversizing ( $\pm 7$  and  $\pm 5\%$ , resp.).<sup>35</sup> In particular, 75%-diastolic phase area and diameter measurements led to (theoretical) undersizing in 15 (14%) and 6 (6%) patients. In this phase, the area and perimeter-derived diameters differed  $2.7 \pm 1.4$  and  $2.0 \pm 1.1$  mm with the prosthesis compared with  $1.5 \pm 1.2$  and  $1.1 \pm 1.2$  mm during maximal phase measurements, respectively. Likewise, Wilsson *et al.* found diastolic phase measurements to result in smaller Sapien XT prostheses in 13/66 patients and in larger in only 1/66 patients.<sup>30</sup> The patients with downsized prostheses showed significant larger conformational change in annulus diameter, area and perimeter compared with patients without a switch in prosthesis size. In contrast, the use of the diastolic diameter in another study resulted in a larger prosthesis in 2/34 patients (29 vs. 26 mm Corevalve).<sup>17</sup> Some patients might show the largest area in the diastolic phase, as also found by de Heer *et al.*<sup>24</sup> in 3/15 patients.

## Discussion

This systematic review clearly demonstrates that the aortic annulus does undergo dynamic conformational change during the cardiac cycle. The annulus becomes more circular in systole and has a predominantly oval shape in diastole. Using double oblique reconstructions perpendicular to the centre lumen line of the left ventricular outflow tract the annulus has a significantly larger short-axis diameter, area, and perimeter in systole compared with diastole. A greater diameter is also found in systolic compared with diastolic phase on the parasternal long-axis and sagittal views, though each was statistically confirmed only by one study. In contrast, the double oblique long-axis diameter suggests no significant change throughout the cardiac cycle and the same goes for the coronal diameter.

**Table 1** Study characteristics

Author (ref)	Year	Patient population	No aortic stenosis		
			N patients	Mean age ± SD	N males (%)
Burman et al. <sup>18</sup>	2008	Healthy subjects	120	49.3 ± 17.2 <sup>a</sup>	60 (50%)
de Heer et al. <sup>10</sup>	2011	CAD screening	108	56.1 ± 12.5	89 (82%)
Kazui et al. <sup>20</sup>	2006	Normal aortic root/valve	25	60.1 ± 14.8	17 (68%)
Martin et al. <sup>31</sup>	2013	Cardiac murmur/pre-chemotherapy	30	11 ± 3.6	NA
de Paulis et al. <sup>13</sup>	2001	Normal aortic root/valve	7	45.3 ± 19	6 (86%)
Veronesi et al. <sup>16</sup>	2009	Normal aortic root/valve	24	54 ± 20	7 (29%)
Zhu et al. <sup>21</sup>	2011	Healthy subjects	314	37.2 ± 13.5	133 (42%)
de Heer et al. <sup>24</sup>	2012	CAD screening vs. TAVI indicated	15	53 ± 12	12 (80%)
Hamdan et al. <sup>33</sup>	2012	CAD screening vs. TAVI indicated	11	56.2 ± 11.8	5 (45%)
Izumi <sup>22</sup>	2012	Pre-AF ablation vs. AS	37	68 ± 5	10 (27%)
Otani et al. <sup>43</sup>	2010	TEE indicated non-AS vs. AS	80	70 ± 10	43 (54%)
Shabestari et al. <sup>32</sup>	2013	CAD screening vs. aortic calcification	52	50.5 ± 11.3	27 (26%)
Shiran et al. <sup>14</sup>	2009	TEE non-AS vs. AS	30	62 ± 13	18 (60%)
Tops et al. <sup>8</sup>	2008	CAD screening no/mild AS vs. AS	150	54 ± 11 <sup>b</sup>	111 (66%) <sup>b</sup>
Tsang et al. <sup>26</sup>	2013	Stroke work-up vs. TAVI indicated	16	80 ± 5	7 (44%)
Tsang et al. <sup>15</sup>	2013	Normal valves vs. AS	20	59.2 ± 17	10 (50%)
Yoshikawa et al. <sup>23</sup>	2013	Stroke work-up vs. AS	40	65.1 ± 11.7	24 (60%)
Bertaso et al. <sup>17</sup>	2012	TAVI indicated	–	–	–
Blanke et al. <sup>35</sup>	2012	TAVI indicated	–	–	–
Bolen et al. <sup>27</sup>	2012	TAVI indicated	–	–	–
Jilaihawi et al. <sup>25</sup>	2012	TAVI indicated	–	–	–
Kempfert et al. <sup>44</sup>	2012	Pre-conventional AVR	–	–	–
Lehmkuhl et al. <sup>28</sup>	2013	TAVI indicated	–	–	–
Lehmkuhl et al. <sup>34</sup>	2013	TAVI indicated	–	–	–
Masri et al. <sup>42</sup>	2014	Pre-TAVI or conventional AVR	–	–	–
Peng et al. <sup>36</sup>	2012	Severe AS	–	–	–
Pontone et al. <sup>29</sup>	2011	TAVI indicated	–	–	–
Willson et al. <sup>30</sup>	2012	TAVI indicated	–	–	–
Wood et al. <sup>19</sup>	2009	TAVI indicated	–	–	–

AVA(i), aortic valve area(indexed); AS, aortic stenosis; CAD, coronary artery disease; CT, computed tomography; NA, not available; HU, CT Hounsfield units; MRI, magnetic resonance imaging; PG, pressure gradient; SD, standard deviation; TAVI, transcatheter aortic valve implantation; TEE, transesophageal echocardiography; TTE, transthoracic echocardiography.

<sup>a</sup>Of male subjects.

<sup>b</sup>Of total group (n = 169).

<sup>c</sup>Of total group (n = 52).

<sup>d</sup>2D speckle tracking echocardiography.

<sup>e</sup>Of total group (n = 96).

<sup>f</sup>Of total group (n = 120).

Results on differences for the magnitude of conformational changes between AS and non-AS patients are contradictory.

The finding that the aortic annulus undergoes conformational changes during the cardiac cycle is important and may add to improved prosthesis design. In clinical setting, this knowledge may add in selecting the optimal imaging phase and approximating the true annular dimensions. Blanke et al. showed better annular agreement with prosthetic sizes selected based on the maximal annular values throughout the cardiac cycle compared with prostheses based on routine predefined systolic (35%) or diastolic (75%) reconstructions.<sup>35</sup> Importantly, de Heer et al. found the cardiac phase

for maximal annulus area to vary between patients from 0–60 and 90% of the RR-interval and similar differences exist for the minimal area.<sup>24</sup> Apparently, the systolic phase does not represent the aortic annulus in its maximal dimensions in all patients. This might also be one of the reasons why some studies found larger diastolic diameters and/or no significant differences in the overall patient group. Assessment of the full cardiac cycle hence enables selection of the annulus in its ultimate dimensions, which may improve the annulus to prosthesis agreement.

Likewise, the choice of the measured parameter may affect prosthesis size selection as well since the annulus, in general, is an

Aortic stenosis			Definition stenosis	AVA (cm <sup>2</sup> )	Mean gradient	Modality
N patients	Mean age ± SD	N males (%)				
–	–	–	–	–	–	MRI
–	–	–	–	–	–	CT
–	–	–	–	–	–	CT
–	–	–	–	–	–	TTE-2D-3D
–	–	–	–	–	–	TEE-2D
–	–	–	–	–	–	TEE-3D
–	–	–	–	–	–	TTE-2D
20	81 ± 6	6 (30%)	Not defined	NA	39 ± 14	CT
35	80.1 ± 7.4	16 (46%)	Not defined	NA	NA	CT
23	73 ± 5	10 (43%)	Not defined	NA	NA	TTE-3D
71	73 ± 8	41 (58%)	Not defined	1.1 ± 0.4	38 ± 20	TEE-3D
30	66.58 ± 8.90 <sup>c</sup>	30 (58%) <sup>c</sup>	Aortic valve calcifications > 100 HU	NA	NA	CT
20	78 ± 9	5 (25%)	Not defined	NA	NA	TTE-2D, TEE-2D
17	54 ± 11 <sup>b</sup>	111 (66%) <sup>b</sup>	Moderate-to-severe AS	0.8 ± 0.2	50 ± 21	CT
27	82 ± 7	16 (59%)	AVA < 1.0 cm <sup>2</sup> , mean PG > 40 mmHg	0.7 ± 0.1	40 ± 12	TEE-3D
20	72 ± 9	14 (70%)	AVA < 1.0 cm <sup>2</sup> , mean PG > 40 mmHg	0.9 ± 0.2	47 ± 11	TEE-3D
40	69.3 ± 9.6	25 (63%)	AVA < 1.0 cm <sup>2</sup> or PG > 40 mmHg	0.8 ± 0.4	43.2 ± 18.4	TEE-2D <sup>d</sup>
59	82.4 ± 5	29 (49%)	AVA < 1 cm <sup>2</sup> , AVAi < 0.6 cm <sup>2</sup> /m <sup>2</sup>	0.7 ± 0.2	NA	CT
110	82.9 ± 7.9	27 (25%)	Severe AS	0.7 ± 0.2	43.6 ± 14.1	CT
47	78 ± 9.5	25 (53%)	Not defined	CT:0.9 ± 0.2	NA	CT
20	84.9 ± 7.2 <sup>e</sup>	50 (52%) <sup>e</sup>	Not defined	NA	NA	CT
26	NA	NA	Severe AS	NA	NA	TTE-2D, TEE-2D
56	81.6 ± 6.8	16 (29%)	Severe AS	0.91 ± 0.14	NA	CT
27	82.3 ± 11.2	6 (22%)	Severe AS	NA	NA	CT
87	81 ± 10	47 (54%)	Symptomatic severe AS	0.6 ± 0.1	46 ± 13	CT
62	68.2 ± 5.9	41 (66%)	Not defined	0.8 ± 0.2	61.6 ± 20.9	CT
60	80 ± 8	22 (37%)	Not defined	0.7 ± 0.2	51.9 ± 15.2	CT
66	81.4 ± 7.8 <sup>f</sup>	57 (48%) <sup>f</sup>	Not defined	0.7 ± 0.2 <sup>f</sup>	42.9 ± 16.6 <sup>f</sup>	CT
19	83.5	NA	Symptomatic severe AS	0.6	50.7	CT

ellipsoid structure. The results show the minimal short diameter axis to significantly change in dimension, whereas the maximal diameter remains relatively unchanged. In addition, the perimeter changes throughout the cardiac cycle as well. These findings support the belief that the annular structure becomes less oval throughout the cycle. Studies using a so-called effective diameter, the diameter calculated from the measured area or perimeter, may induce an error if solely formulas for circular structures are applied. Evaluation of multiple parameters may be desirable in specific patients, for instance, in patients whose annular dimensions are in the overlapping/ borderzone prosthesis size recommendations. Multiphase assessment providing knowledge on the amount of annular distensibility may also be helpful in choosing the most optimal size in these patients.

Furthermore, the change in dimensions of the aortic annulus seems to urge the use of three-dimensional techniques for accurate annulus size assessment. Table 7 provides an overview of current imaging modalities used for annulus measurements. An advantage of CT is that it provides an overview of the cardiac anatomy and

calcifications present which may impact prosthesis size selection in borderzone patients.<sup>37</sup> TEE might be a helpful three-dimensional modality in patients not eligible for contrast-enhanced CT imaging.<sup>37–39</sup> However, compared with CT measurements 3D-TEE consistently displayed smaller dimensions, which may cause significant undersizing.<sup>38,39</sup> Two-dimensional TEE showed even more undersizing compared with CT-based sizing.<sup>39</sup> Hence, the use of three-dimensional imaging modalities and CT in particular seems indispensable to reduce potential sizing error.

Patient post-procedural outcome has often been related to the presence of relevant paravalvular regurgitation, although the direct association with mortality yet needs to be evaluated.<sup>40</sup> One of the key factors in paravalvular regurgitation is the relation with prosthesis oversizing and undersizing.<sup>28,30,41</sup> The purpose of this review was to assess whether the aortic annulus undergoes significant dynamic change and its possible implications for prosthesis size selection. Currently, TAVI prostheses are available in four sizes (23, 26, 29, and 31 mm) for annular sizes of 18–29 mm and the prosthesis size recommendations overlap for annulus dimensions.

**Table 2** Parasternal long-axis annulus diameter measurements

Author	Imaging	Cardiac phase measured	Systole	Diastole	Mean difference	P-value
Patients without aortic valve stenosis						
Kazui et al. <sup>20</sup>	CT <sup>a</sup>	40%, 80% RR-interval	22.5 ± 2.2	22.1 ± 2.2	–	NS
Martin et al. <sup>31</sup>	TTE-2D	Mid-systole, end-diastole	19.4	19.5	–	–
de Paulis et al. <sup>13</sup>	TEE-2D	Systole, diastole	22.2 ± 1.6	20.6 ± 1	7 ± 3.2%	–
Shiran et al. <sup>b14</sup>	TTE-2D	Mid-systole, end-diastole	21.1 ± 2.1	21.0 ± 1.8	0.2 ± 0.8	P = 0.2
	TEE-2D	Mid-systole, end-diastole	21.6 ± 2.2	21.3 ± 2.1	0.3 ± 0.7	P = 0.0005
Yoshikawa et al. <sup>23</sup>	TEE-2D <sup>c</sup>	83 ms, 421 ms from ECG R-wave	22.9 ± 2.7	20.0 ± 2.9	2.9 ± 0.7	–
Zhu et al. <sup>21</sup>	TTE-2D	Mid-systole, end-diastole	20.91 ± 2.29	20.35 ± 8.67	–	–
Patients with aortic valve stenosis						
Kempfert et al. <sup>44</sup>	TTE-2D	End-systole, end-diastole	24.2 ± 3.5	22.9 ± 3.1	–	–
	TEE-2D	End-systole, end-diastole	24.5 ± 2.7	23.8 ± 2.7	–	–
Yoshikawa et al. <sup>23</sup>	TEE-2D <sup>c</sup>	99 ms, 435 ms from ECG R-wave	21.6 ± 2.6	19.4 ± 2.6	2.2 ± 0.6	–

All annular measurements are presented in millimetres as mean ± SD.

CT, computed tomography; NS, non-significant; ms, milliseconds; TEE, transesophageal echocardiography; TTE, transthoracic echocardiography.

<sup>a</sup>In CT longitudinal view.

<sup>b</sup>Results are similar for stenosis patients.

<sup>c</sup>TEE speckle tracing.

**Table 3** Coronal and sagittal-axis annulus diameter measurements

Author	Imaging	Cardiac phase measured	Coronal view		Mean Δ	P-value	Sagittal view		Mean Δ	P-value
			Systole	Diastole			Systole	Diastole		
Patients without aortic valve stenosis										
Burman et al. <sup>18</sup>	MRI	Max systolic, end-diastolic	25.7 ± 2.1 (M)	26.2 ± 2.3	–	–	22.4 ± 2.1	22.2 ± 2.4	–	–
			23.0 ± 2.0 (F)	23.0 ± 2.1	–	–	21.0 ± 2.1	19.9 ± 1.9	–	–
de Heer et al. <sup>10</sup>	CT	30–40%, 70–75% RR-interval	26.6 ± 2.8	26.9 ± 2.4	–	–	–	–	–	–
Tops et al. <sup>8</sup>	CT	30%, 75% RR-interval	26.4 ± 2.8	26.3 ± 2.6	–	–	24.0 ± 2.6	23.4 ± 2.7	–	–
Patients with aortic valve stenosis										
Bertaso et al. <sup>17</sup>	CT	30–40%, 70–80% RR-interval	25.3 ± 2.7	25.5 ± 2.7	0.23 (0.9%)	0.115	22 ± 2.4	21.6 ± 2.3	0.42 (1.9%)	0.008
Tops et al. <sup>8</sup>	CT	30%, 75% RR-interval	27.3 ± 3.7	26.7 ± 3.9	–	–	24.7 ± 3.0	24.2 ± 3.0	–	–
Wood et al. <sup>19</sup>	CT	30%, 70% RR-interval	25.7 ± 1.5	25.5 ± 2.5	–	–	22.4 ± 1.3	21.5 ± 2.1	–	–

All annular measurements are presented in millimetres as mean ± SD.

F, females; M, males.

Mean Δ = mean difference between systolic and diastolic measurement.

Results showed the systolic short-axis diameter to differ significantly by (mean) 0.75 mm minimum<sup>17</sup> to 2.7 ± 1.6 mm maximum<sup>33</sup> from the diastolic diameter. Maximal differences within the cycle ranged to even 8.7 mm in Peng et al.<sup>36</sup> With little annular change, the impact on TAVI sizing may be small as was the case in the study of Bertaso et al.<sup>17</sup> With greater annular deformations, diastolic sizing can lead to a relevant change in prosthetic size selection, as 20% of patients in the study of Willson et al. received a smaller prosthesis.<sup>30</sup> The conformational change of the annulus showed to impact the annulus to prosthesis agreement,<sup>35</sup> consequently it also may result in (undesired) oversizing or undersizing and thus in paravalvular leakage. Remarkably, one study found significantly less conformational

change of the annulus in patients with clinically relevant paravalvular leakage, showing a mean area deformation of 32 ± 10 vs. 46 ± 21 mm<sup>2</sup> (P = 0.003) in non-leakage patients and perimeter deformation of 2.6 ± 0.8 vs. 3.6 ± 1.3 mm (P = 0.001), respectively.<sup>42</sup> For paravalvular leakage prediction, the same study showed 74% sensitivity and 72% specificity for conformational changes of <3 mm in annular perimeter. Prosthesis to annular perimeter size ratio and annular calcifications were also independent predictors for paravalvular leakage.

As shown in this review, results vary remarkably between specific studies. The reported mean percentage change ranges from 4 to 28% for area, 2–12% for minimal diameter and 0.56–7.3%

**Table 4** Double oblique plane annulus diameter measurements

Author	Imaging	Cardiac phase measured	Maximal diameter				Minimal diameter			
			Systole	Diastole	Mean Δ	P-value	Systole	Diastole	Mean Δ	P-value
Patients without aortic valve stenosis										
Hamdan <i>et al.</i> <sup>33</sup>	CT	All: max 30%, min 90–0%	–	–	–	–	21.7 ± 1.8	19.0 ± 2.6	12.3 ± 7.3%	<0.001
de Heer <i>et al.</i> <sup>10</sup>	CT	30–40%, 70–75%	29.7 ± 3.4	30.1 ± 3.0	0.3 ± 2.4	<0.001	25.1 ± 3.3	24.0 ± 3.1	1.1 ± 2.0	<0.001
Izumi <i>et al.</i> <sup>22</sup>	TTE-3D	End-systole, end-diastole	–	–	–	–	20.6 ± 1.4	22.4 ± 1.6	7.8 ± 3.4%	<0.0001
Martin <i>et al.</i> <sup>31</sup>	TTE-3D	Mid-systole, end-diastole	20.1	20.1	–	–	18.8	19.3	–	–
Otani <i>et al.</i> <sup>43</sup>	TEE-3D	Mid-systole, end-diastole	24.6 ± 2.1	25.0 ± 2.2	–	–	19.6 ± 1.8	19.1 ± 1.8	–	–
Shabestari <i>et al.</i> <sup>32</sup>	CT	30–35%, 70–75%	26.69 ± 2.72	27.85 ± 3.09	0.59	–	20.80 ± 2.47	20.86 ± 1.81	0.05	–
Patients with aortic valve stenosis										
Bertaso <i>et al.</i> <sup>17</sup>	CT	30–40%, 70–80%	28.7 ± 2.7	28.4 ± 2.7	0.24 (0.7%)	0.163	22.4 ± 2.4	21.7 ± 2.4	0.75 (3.4%)	0.004
Blanke <i>et al.</i> <sup>35</sup>	CT	All: max 20%, min 60%	27.8 <sup>a</sup>	26.8 <sup>a</sup>	2%	–	22.0 ± 1.9	19.8 <sup>a</sup>	11%	–
Bolen <i>et al.</i> <sup>27</sup>	CT	20–30%, 90%	28.4 ± 3.5	28.7 ± 3.4	–	0.67	22.9 ± 2.4	21.4 ± 2.5	–	0.006
Hamdan <i>et al.</i> <sup>33</sup>	CT	All: max 30%, min 90–0%	–	–	–	–	22.6 ± 2.9	20.4 ± 2.7	9.8 ± 3.4%	<0.001
Izumi <i>et al.</i> <sup>22</sup>	TTE-3D	End-systole, end-diastole	–	–	–	–	18.7 ± 1.9	19.1 ± 1.7	2.0 ± 2.2%	<0.0001
Jilaihawi <i>et al.</i> <sup>25</sup>	CT	Mean at 16% and 54%	27.1 ± 2.9	26.8 ± 2.8	–	0.43	21.3 ± 2.7	19.7 ± 2.3	–	<0.0001
Lehmkuhl <i>et al.</i> <sup>28</sup>	CT	40–50%, 90–0%	27.1 ± 3 <sup>b</sup>	27.0 ± 3.0 <sup>b</sup>	1.6 ± 1.2	NS	24.8 ± 2.9 <sup>c</sup>	23.0 ± 3.2 <sup>c</sup>	2.2 ± 1.6	<0.001
Lehmkuhl <i>et al.</i> <sup>34</sup>	CT	End-systole, end-diastole	24.7 ± 2.2 <sup>b</sup>	24.8 ± 2.0 <sup>b</sup>	–	–	21.4 ± 1.8 <sup>c</sup>	20.5 ± 2.0 <sup>c</sup>	1.2 ± 2.0	<0.01
Masri <i>et al.</i> <sup>42</sup>	CT	All: max NA, min NA	26 ± 3	25 ± 3	1.2 ± 0.5	–	21 ± 3	20 ± 3	1.2 ± 0.5	–
Otani <i>et al.</i> <sup>43</sup>	TEE-3D	Mid-systole, end-diastole	25.2 ± 2.8	25.2 ± 2.6	–	–	19.5 ± 2.3	19.2 ± 2.3	–	–
Peng <i>et al.</i> <sup>36</sup>	CT	All: max 0–10%, min 50%	28.2 ± 4.0	27.1 ± 3.7	3.2 ± 1.4	–	23.1 ± 2.6	21.1 ± 2.8	3.6 ± 1.4	–
Pontone <i>et al.</i> <sup>29</sup>	CT	Systole, diastole	25.1 ± 2.8	25.4 ± 2.7	–	NS	21.2 ± 2.2	20.1 ± 2.7	–	NS
Shabestari <i>et al.</i> <sup>32</sup>	CT	30–35%, 70–75%	27.16 ± 3.11	27.42 ± 2.62	–	–	20.57 ± 2.10	20.45 ± 2.37	–	–
Willson <i>et al.</i> <sup>30</sup>	CT	25–35%, 75%	26.6 ± 2.84	26.2 ± 2.90	–	0.22	20.8 ± 2.24	20.2 ± 1.99	–	0.01

All annular measurements are presented in millimetres as mean ± SD.

<sup>a</sup>Derived from graphs.

<sup>b</sup>Distance between basal attachment of left coronary cusp and opposite intercommissure.

<sup>c</sup>Distance between basal attachment of right coronary cusp and opposite intercommissure.

**Table 5** Double oblique plane annulus area measurements

Author	Imaging	Cardiac phase measured	Area method	Area systole	Diastole	P-value	Mean difference	P-value
Patients without aortic valve stenosis								
De Heer <i>et al.</i> <sup>24</sup>	CT	All: max 0–30%, min 50–70%	Semi-automatic	NA	NA	–	122 ± 33 (28 ± 10%)	<0.001
Veronesi <i>et al.</i> <sup>16</sup>	TEE-3D	All: max 19%, min 57%	Semi-automatic	3.7 ± 1.1*	4.6 ± 1.3*	<0.05	–	–
Hamdan <i>et al.</i> <sup>33</sup>	CT	All: max 30%, min 90–0%	Manual	448 ± 81.8	398.7 ± 93.7	<0.001	11.2 ± 5.2%	<0.001
Otani <i>et al.</i> <sup>43</sup>	TEE-3D	Mid-systole, end-diastole	Manual	391 ± 66	390 ± 65	–	–	–
Shabestari <i>et al.</i> <sup>32</sup>	CT	30–35%, 70–75%	Manual	457.71 ± 82.86	460.24 ± 79.70	–	2.53	–
Tsang <i>et al.</i> <sup>26</sup>	TEE-3D	All: max NA, min NA	Semi-automatic	5.3 ± 1.1*	4.2 ± 1.1*	–	–	–
Tsang <i>et al.</i> <sup>15</sup>	TEE-3D	All: max NA, min NA	semi-automatic	5.4 ± 1.0*	4.4 ± 1.2*	–	–	–
Patients with aortic valve stenosis								
De Heer <i>et al.</i> <sup>24</sup>	CT	All: max 0–30%, min 50–70%	Semi-automatic	NA	NA	–	98 ± 52 (21 ± 10%)	<0.001
Hamdan <i>et al.</i> <sup>33</sup>	CT	All: max 30%, min 90–0%	Manual	480.9 ± 108	438.8 ± 103	<0.001	6.2 ± 4.8%	<0.001
Otani <i>et al.</i> <sup>43</sup>	TEE-3D	Mid-systole, end-diastole	Manual	397 ± 89	396 ± 88	–	–	–
Shabestari <i>et al.</i> <sup>32</sup>	CT	30–35%, 70–75%	Manual	437.82 ± 92.44	438.31 ± 79.25	–	6.92	–
Bertaso <i>et al.</i> <sup>17</sup>	CT	30–40%, 70–80%	Ellipse equation	509 ± 12	488 ± 12	–	4%	0.002
Blanke <i>et al.</i> <sup>35</sup>	CT	All: max 20%, min 60%	Manual	483.4 ± 75.2	410.5 ± 68.7	<0.001	72.9 ± 22.6 (18.2%)	<0.001
Masri <i>et al.</i> <sup>42</sup>	CT	All: max NA, min NA	Manual	482 ± 111	445 ± 102	–	38 ± 17	–
Pontone <i>et al.</i> <sup>29</sup>	CT	Systole, diastole	Manual	410.5 ± 81.4	409.2 ± 97.1	NS	–	–
Tsang <i>et al.</i> <sup>26</sup>	TEE-3D	All: max NA, min NA	Semi-automatic	4.4 ± 1.4*	3.8 ± 1.2*	–	–	–
Tsang <i>et al.</i> <sup>15</sup>	TEE-3D	All: max NA, min NA	Semi-automatic	5.1 ± 1.1*	3.7 ± 1.7*	–	–	–
Willson <i>et al.</i> <sup>30</sup>	CT	25–35%, 75%	Manual	4.7 ± 0.8*	4.5 ± 0.9*	<0.001	–	–

Measurements are presented in square millimetre or square centimetre if indicated with \* as mean ± SD. NA, not available; NS, not significant.



**Table 6** Double oblique plane annulus perimeter measurements

Author	Imaging	Cardiac phase measured	Perimeter			P-value
			Systole	Diastole	Mean difference	
Patients without aortic valve stenosis						
Hamdan <i>et al.</i> <sup>33</sup>	CT	All: max 30%, min 90–0%	76.1 ± 6.7	74.1 ± 7.6	2.2 ± 2.2%	0.01
Shabestari <i>et al.</i> <sup>32</sup>	CT	30–35%, 70–75%	86.64 ± 7.40	88.12 ± 8.90	1.48	–
Veronesi <i>et al.</i> <sup>16</sup>	TEE-3D	All: max 19%, min 57%	69.5 ± 10.6	78.1 ± 11.5	–	<0.05
Patients with aortic valve stenosis						
Blanke <i>et al.</i> <sup>35</sup>	CT	All: max 20%, min 60%	79.6 ± 6.0	74.2 ± 5.7	5.4 ± 1.5(7.3 ± 2.1%)	<0.001
Hamdan <i>et al.</i> <sup>33</sup>	CT	All: max 30%, min 90–0%	78.9 ± 8.7	77.3 ± 8.6	0.56 ± 0.85%	0.01
Masri <i>et al.</i> <sup>42</sup>	CT	All: max NA, min NA	80 ± 9	77 ± 9	3 ± 1	–
Shabestari <i>et al.</i> <sup>32</sup>	CT	30–35%, 70–75%	86.67 ± 8.52	87.51 ± 8.21	–	–
Willson <i>et al.</i> <sup>30</sup>	CT	25–35%, 75%	78.5 ± 8.2	77.2 ± 8.0	–	0.01

All measurements are presented in millimetres as mean ± SD.  
NA, not available.

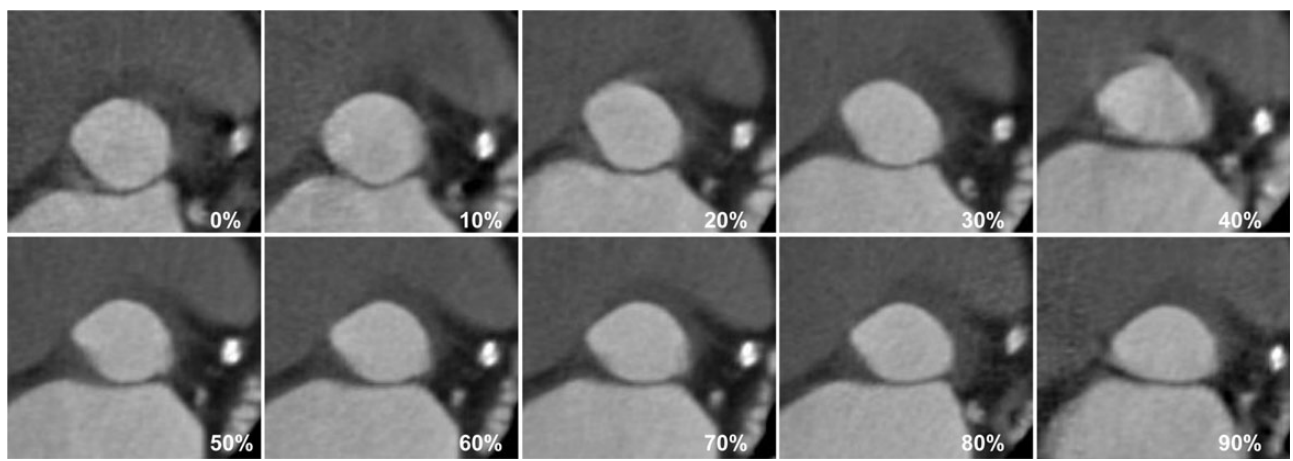


**Figure 2** Dynamic deformation of the annulus. Cardiac ECG-gated multidetector-row computed tomography images reconstructed in each 10% phase of the RR-interval. Note the conformational change of the aortic annulus showing a more circular shape during systole and an oval shape during diastole. Whereas the long-axis diameter remains relatively stable, the short-axis diameter undergoes significant change throughout the cycle.

perimeter. Evidently, the heterogeneity between studies is substantial and likely accounts for the observed ranges. Significant differences are present for both study methods and patient characteristics. With regard to the first, study sample size and imaging modality may affect study results just like the assessment of two predefined vs. all cardiac phases and manual vs. semi-automatic measurements. Second, patient age, gender, and degree and/or definition of stenosis differ between studies. The impact of gender on the amount of conformational change has not been evaluated and only one study reported on the effect of age without significant differences. No consensus exists on whether the annular conformational changes vary between AS patients and non-AS patients. Furthermore, patients with aortic root calcifications in general did

not show significant differences with the control group, whereas significant differences were found for annular area related to the distribution of calcifications.<sup>32</sup> More research and larger study samples are needed to provide basic insight on various potential factors affecting the annular distensibility and conformational changes. As for TAVI sizing and patient outcome, it is essential to take the dynamic deformation into consideration by selecting the optimal imaging modality, cardiac phase, and annular parameter. Based on this review, we can conclude that three-dimensional imaging is required for adequate annulus assessment. Despite its well-known drawbacks, CT provides the most comprehensive overview of cardiac structures and optimal imaging plane reconstructions and hence allows for reliable assessment of all annular dimensions. The use of

**Table 7** Imaging modalities

Imaging	Benefits	Drawbacks
2D-TTE	Non-invasive Readily available and portable No contrast agent required	Operator dependent Two-dimensional assessment Image quality limited (acoustic shadowing, obesity, and chronic obstructive pulmonary disease)
2D-TEE	High spatial resolution No contrast agent required Intra-operative use possible	Semi-invasive Operator dependent Two-dimensional assessment Possible complications Might require sedation Specific contraindications (oesophageal disease)
3D-TEE	Three-dimensional assessment No contrast agent required Intra-operative use possible	Semi-invasive Operator dependent Possible complications Might require sedation Specific contraindications (oesophageal disease)
CT	High spatial resolution Non-invasive Three-dimensional assessment Short acquisition time Anatomic overview Allows calcium (distribution) assessment	Contrast agent required Radiation exposure Heart rate control may be required Specific contraindications (pregnancy, impaired renal function, and contrast allergy)
MRI	High contrast resolution Non-invasive Three-dimensional assessment Anatomic overview	Long acquisition time Patient breath holding Specific contraindications (claustrophobia, metal implants, and pacemakers, haemodynamic instability)

2D-TTE, two-dimensional transthoracic echocardiography; 2D-TEE, two-dimensional transesophageal echocardiography; 3D-TEE, three-dimensional transesophageal echocardiography; CT, computed tomography; MRI, magnetic resonance imaging.

two-dimensional imaging modalities on the other hand may lead to relevant prosthesis undersizing. Furthermore, selection of the cardiac phase in which the annulus shows the largest dimensions seems to prevent (theoretical) prosthesis undersizing, but the maximal phase is patient specific. Future studies are required to evaluate the effect of the use of different annular parameters on patient outcome and to prospectively assess the clinical impact of sizing based on different cardiac phases.

## Limitations

In this study, we did not take the effect of semi-automatic or manual measurements into account. Secondly, variability in the definition of annulus might impact study results, although the majority of included studies (76%) used the same definition. Thirdly, published results lack data on paired intra-patient analyses to be able to assess differences on patient level. Lumping the mean overall systolic and diastolic diameters reported will not provide the mean difference within patients. Hence, insufficient data were available to perform a meta-analysis to acquire the pooled difference for mean change of the annulus within the cardiac cycle. Finally, evaluation of the accuracy of annulus measurements using different imaging modalities in comparison with true intra-operative measurements was beyond the scope of this review.

**Conflict of interest:** None declared.

## References

- Go AS, Mozaffarian D, Roger VL, Benjamin EJ, Berry JD, Baha MJ et al. Heart disease and stroke statistics – 2014 update: a report from the American Heart Association. *Circulation* 2014;**129**:e28–e292.
- Bach DS. Prevalence and characteristics of unoperated patients with severe aortic stenosis. *J Heart Valve Dis* 2011;**20**:284–91.
- Kodali SK, Williams MR, Smith CR, Svensson LG, Webb JG, Makkar RR et al. Two-year outcomes after transcatheter or surgical aortic-valve replacement. *N Engl J Med* 2012;**366**:1686–95.
- Toggweiler S, Humphries KH, Lee M, Binder RK, Moss RR, Freeman M et al. 5-year outcome after transcatheter aortic valve implantation. *J Am Coll Cardiol* 2013;**61**:413–9.
- Jerez-Valero M, Urena M, Webb JG, Tamburino C, Munoz-Garcia AJ, Cheema A et al. Clinical impact of aortic regurgitation after transcatheter aortic valve replacement: insights into the degree and acuteness of presentation. *JACC Cardiovasc Interv* 2014;**7**:1022–32.
- Chrysohoou C, Hayek SS, Spiliadis N, Lerakis S. Echocardiographic and clinical factors related to paravalvular leak incidence in low-gradient severe aortic stenosis patients post-transcatheter aortic valve implantation. *Eur Heart J Cardiovasc Imaging* 2015;**16**:558–63.
- O'Sullivan KE, Gough A, Segurado R, Barry M, Sugrue D, Hurley J. Is valve choice a significant determinant of paravalvular leak post-transcatheter aortic valve implantation? A systematic review and meta-analysis. *Eur J Cardiothorac Surg* 2014;**45**:826–33.
- Tops LF, Wood DA, Delgado V, Schuijff JD, Mayo JR, Pasupati S et al. Noninvasive evaluation of the aortic root with multislice computed tomography implications for transcatheter aortic valve replacement. *JACC Cardiovasc Imaging* 2008;**1**:321–30.
- Messika-Zeitoun D, Serfaty JM, Brochet E, Ducrocq G, Lepage L, Detaint D et al. Multimodal assessment of the aortic annulus diameter: Implications for transcatheter aortic valve implantation. *J Am Coll Cardiol* 2010;**55**:186–94.
- de Heer LM, Budde RP, Mali WP, de Vos AM, van Herwerden LA, Kluijn J. Aortic root dimension changes during systole and diastole: Evaluation with ecg-gated multidetector row computed tomography. *Int J Cardiovasc Imaging* 2011;**27**:1195–204.

11. Albano AJ, Mitchell E, Pape LA. Standardizing the method of measuring by echocardiogram the diameter of the ascending aorta in patients with a bicuspid aortic valve. *Am J Cardiol* 2010;**105**:1000–4.
12. van Prehn J, Vincken KL, Muhs BE, Barwegen GK, Bartels LW, Prokop M *et al*. Toward endografting of the ascending aorta: insight into dynamics using dynamic cine-cta. *J Endovasc Ther* 2007;**14**:551–60.
13. De Paulis R, De Matteis GM, Nardi P, Scaffa R, Buratta MM, Chiariello L. Opening and closing characteristics of the aortic valve after valve-sparing procedures using a new aortic root conduit. *Ann Thorac Surg* 2001;**72**:487–94.
14. Shiran A, Adawi S, Ganaem M, Asmer E. Accuracy and reproducibility of left ventricular outflow tract diameter measurement using transthoracic when compared with transesophageal echocardiography in systole and diastole. *Eur J Echocardiogr* 2009;**10**:319–24.
15. Tsang W, Veronesi F, Sugeng L, Weinert L, Takeuchi M, Jeevanandam V *et al*. Mitral valve dynamics in severe aortic stenosis before and after aortic valve replacement. *J Am Soc Echocardiogr* 2013;**26**:606–14.
16. Veronesi F, Corsi C, Sugeng L, Mor-Avi V, Caiani EG, Weinert L *et al*. A study of functional anatomy of aortic-mitral valve coupling using 3d matrix transesophageal echocardiography. *Circ Cardiovasc Imaging* 2009;**2**:24–31.
17. Bertaso AG, Wong DT, Liew GY, Cunningham MS, Richardson JD, Thomson VS *et al*. Aortic annulus dimension assessment by computed tomography for transcatheter aortic valve implantation: Differences between systole and diastole. *Int J Cardiovasc Imaging* 2012;**28**:2091–8.
18. Burman ED, Keegan J, Kilner PJ. Aortic root measurement by cardiovascular magnetic resonance: Specification of planes and lines of measurement and corresponding normal values. *Circ Cardiovasc Imaging* 2008;**1**:104–13.
19. Wood DA, Tops LF, Mayo JR, Pasupati S, Schlij MJ, Humphries K *et al*. Role of multislice computed tomography in transcatheter aortic valve replacement. *Am J Cardiol* 2009;**103**:1295–301.
20. Kazui T, Izumoto H, Yoshioka K, Kawazoe K. Dynamic morphologic changes in the normal aortic annulus during systole and diastole. *J Heart Valve Dis* 2006;**15**: 617–21.
21. Zhu D, Zhao Q. Dynamic normal aortic root diameters: implications for aortic root reconstruction. *Ann Thorac Surg* 2011;**91**:485–9.
22. Izumi C, Miyake M, Takahashi S, Hayashi H, Miyanishi T, Matsutani H *et al*. Usefulness of real-time three-dimensional echocardiography in evaluating aortic root diameters during a cardiac cycle. *J Echocardiogr* 2012;**10**:8–14.
23. Yoshikawa H, Suzuki M, Hashimoto G, Kusunose Y, Otsuka T, Hara H *et al*. Assessment of cyclic changes in the diameter of the aortic annulus using speckle-tracking trans-esophageal echocardiography. *Ultrasound Med Biol* 2013;**39**:2084–90.
24. de Heer LM, Budde RP, van Prehn J, Mali WP, Bartels LW, Stella PR *et al*. Pulsatile distention of the nondiseased and stenotic aortic valve annulus: analysis with electrocardiogram-gated computed tomography. *Ann Thorac Surg* 2012;**93**:516–22.
25. Jilalawi H, Kashif M, Fontana G, Furugen A, Shiota T, Friede G *et al*. Cross-sectional computed tomographic assessment improves accuracy of aortic annular sizing for transcatheter aortic valve replacement and reduces the incidence of paravalvular aortic regurgitation. *J Am Coll Cardiol* 2012;**59**:1275–86.
26. Tsang W, Meineri M, Hahn RT, Veronesi F, Shah AP, Osten M *et al*. A three-dimensional echocardiographic study on aortic-mitral coupling in transcatheter aortic valve replacement. *Eur Heart J Cardiovasc Imaging* 2013;**14**:950–6.
27. Bolen MA, Popovic ZB, Dahiya A, Kapadia SR, Tuzcu EM, Flamm SD *et al*. Prospective ecg-triggered, axial 4-D imaging of the aortic root, valvular, and left ventricular structures: a lower radiation dose option for preprocedural TAVR imaging. *J Cardiovasc Comput Tomogr* 2012;**6**:393–8.
28. Lehmkühl L, Foldyna B, Von Aspern K, Lucke C, Grothoff M, Nitzsche S *et al*. Inter-individual variance and cardiac cycle dependency of aortic root dimensions and shape as assessed by ecg-gated multi-slice computed tomography in patients with severe aortic stenosis prior to transcatheter aortic valve implantation: Is it crucial for correct sizing? *Int J Cardiovasc Imaging* 2013;**29**:693–703.
29. Pontone G, Andreini D, Bartorelli AL, Annoni A, Mushtaq S, Bertella E *et al*. Feasibility and accuracy of a comprehensive multidetector computed tomography acquisition for patients referred for balloon-expandable transcatheter aortic valve implantation. *Am Heart J* 2011;**161**:1106–13.
30. Willson AB, Webb JG, Freeman M, Wood DA, Gurvitch R, Thompson CR *et al*. Computed tomography-based sizing recommendations for transcatheter aortic valve replacement with balloon-expandable valves: Comparison with transesophageal echocardiography and rationale for implementation in a prospective trial. *J Cardiovasc Comput Tomogr* 2012;**6**:406–14.
31. Martin R, Hascoet S, Dulac Y, Peyre M, Mejean S, Hadeed K *et al*. Comparison of two- and three-dimensional transthoracic echocardiography for measurement of aortic annulus diameter in children. *Arch Cardiovasc Dis* 2013;**106**:492–500.
32. Shabestari A, Pourghorban R, Tehrai M, Pouraliakbar H, Faghihi Langroudi T, Bakshshandeh H *et al*. Comparison of aortic root dimension changes during cardiac cycle between the patients with and without aortic valve calcification using ecg-gated 64-slice and dual-source 256-slice computed tomography scanners: Results of a multicenter study. *Int J Cardiovasc Imaging* 2013;**29**:1391–400.
33. Hamdan A, Guetta V, Konen E, Goitein O, Segev A, Raanani E *et al*. Deformation dynamics and mechanical properties of the aortic annulus by 4-dimensional computed tomography: insights into the functional anatomy of the aortic valve complex and implications for transcatheter aortic valve therapy. *J Am Coll Cardiol* 2012;**59**: 119–27.
34. Lehmkühl LH, von Aspern K, Foldyna B, Grothoff M, Nitzsche S, Kempfert J *et al*. Comparison of aortic root measurements in patients undergoing transapical aortic valve implantation (TA-AVI) using three-dimensional rotational angiography (3D-RA) and multislice computed tomography (MSCT): Differences and variability. *Int J Cardiovasc Imaging* 2013;**29**:417–24.
35. Blanke P, Russe M, Leipsic J, Reinohl J, Ebersberger U, Suranyi P *et al*. Conformational pulsatile changes of the aortic annulus: impact on prosthesis sizing by computed tomography for transcatheter aortic valve replacement. *JACC Cardiovasc Interv* 2012;**5**:984–94.
36. Peng LQ, Yang ZG, Yu JQ, Chu ZG, Deng W, Shao H. Dynamic assessment of aortic annulus in patients with aortic stenosis throughout cardiac cycle with dual-source computed tomography. *Int J Cardiol* 2012;**158**:304–7.
37. Husser O, Holzamer A, Resch M, Endemann DH, Nunez J, Bodi V *et al*. Prosthesis sizing for transcatheter aortic valve implantation – comparison of three dimensional transesophageal echocardiography with multislice computed tomography. *Int J Cardiol* 2013;**168**:3431–8.
38. Jilalawi H, Doctor N, Kashif M, Chakravarty T, Rafique A, Makar M *et al*. Aortic annular sizing for transcatheter aortic valve replacement using cross-sectional 3-dimensional transesophageal echocardiography. *J Am Coll Cardiol* 2013;**61**:908–16.
39. Ng AC, Delgado V, van der Kley F, Shanks M, van de Veire NR, Bertini M *et al*. Comparison of aortic root dimensions and geometries before and after transcatheter aortic valve implantation by 2- and 3-dimensional transesophageal echocardiography and multislice computed tomography. *Circ Cardiovasc Imaging* 2010;**3**:94–102.
40. Genereux P, Head SJ, Hahn R, Daneault B, Kodali S, Williams MR *et al*. Paravalvular leak after transcatheter aortic valve replacement: The new achilles' heel? A comprehensive review of the literature. *J Am Coll Cardiol* 2013;**61**:1125–36.
41. Willson AB, Webb JG, Labounty TM, Achenbach S, Moss R, Wheeler M *et al*. 3-dimensional aortic annular assessment by multidetector computed tomography predicts moderate or severe paravalvular regurgitation after transcatheter aortic valve replacement: a multicenter retrospective analysis. *J Am Coll Cardiol* 2012;**59**: 1287–94.
42. Masri A, Schoenhagen P, Svensson L, Kapadia SR, Griffin BP, Tuzcu EM *et al*. Dynamic characterization of aortic annulus geometry and morphology with multimodality imaging: Predictive value for aortic regurgitation after transcatheter aortic valve replacement. *J Thorac Cardiovasc Surg* 2014;**147**:1847–54.
43. Otani K, Takeuchi M, Kaku K, Sugeng L, Yoshitani H, Haruki N *et al*. Assessment of the aortic root using real-time 3D transesophageal echocardiography. *Circ J* 2010;**74**:2649–57.
44. Kempfert J, Van Linden A, Lehmkühl L, Rastan AJ, Holzhey D, Blumenstein J *et al*. Aortic annulus sizing: echocardiographic versus computed tomography derived measurements in comparison with direct surgical sizing. *Eur J Cardiothorac Surg* 2012;**42**:627–33.

## Appendix

Search strategy performed in PubMed<sup>a</sup> and Embase<sup>b</sup> on 25 June 2014

- 1 Imaging OR CT OR CTs OR 'computer tomography' OR 'computed tomography' OR 'computerized tomography' OR 'CAT scan' OR 'CAT scans' OR MDCT OR MSCT OR CTA OR 'computer-assisted tomography' OR 'computed-assisted tomography' OR 'magnetic resonance imaging' OR 'magnetic resonance' OR MRI OR MR OR NMR OR NMRI OR CMR OR echocardiographies OR echocardiography OR TTE OR TEE OR ultrasound OR ultrasonographies OR ultrasonography OR ultrasonic OR echography OR echographies OR echotomography OR echotomographies
- 2 'aortic annulus' OR 'aortic annular' OR 'aortic root' OR TAVI OR TAVR OR 'transcatheter valve' OR 'percutaneous valve' OR 'transcatheter aortic valve' OR 'percutaneous aortic valve'
- 3 (1 and 2)

<sup>a</sup>In title/abstract.

<sup>b</sup>In title/abstract: no conference abstract, letter, note, or editorial.